



UNIVERSIDADE FEDERAL DO PARÁ  
FACULDADE DE ENGENHARIA

ANA CAROLINA DE SOUZA ALVES

**WAVE ENERGY UTILIZATION FOR PIPE-IN-PIPE HEATING: A TECHNIQUE  
TO PREVENT HYDRATE FORMATION IN OFFSHORE HYDROCARBON TRANS-  
PORTATION.**

SALINÓPOLIS-PA  
2025



UNIVERSIDADE FEDERAL DO PARÁ  
FACULDADE DE ENGENHARIA

ANA CAROLINA DE SOUZA ALVES

**WAVE ENERGY UTILIZATION FOR PIPE-IN-PIPE HEATING: A TECHNIQUE  
TO PREVENT HYDRATE FORMATION IN OFFSHORE HYDROCARBON TRANS-  
PORTATION.**

Trabalho de Conclusão de Curso apresentado a Faculdade de Engenharia, da Universidade Federal do Pará campus Salinópolis, como requisito para a obtenção do Grau de Bacharel em Engenharia de Exploração e Produção de Petróleo.

Orientador: Prof. Dr. Camilo Guerrero Martin

SALINÓPOLIS-PA  
2025

**ANA CAROLINA DE SOUZA ALVES**

**WAVE ENERGY UTILIZATION FOR PIPE-IN-PIPE  
HEATING: A TECHNIQUE TO PREVENT HYDRATE  
FORMATION IN OFFSHORE HYDROCARBON TRANS-  
PORTATION.**

Trabalho julgado para a obtenção do grau de Engenheiro de Pesca do Curso de Engenharia de Exploração e Produção de Petróleo da Universidade Federal do Pará, Campus de Salinópolis.

Data da avaliação: 18/08/2025

Conceito: 10

**BANCA EXAMINADORA**

---

Prof. Dr. Camilo Guerrero Martin  
UFPA – Orientador

---

Prof. Dr. Vando Costa Gomes  
UFPA – Membro titular



---

Msc (C). Laura Estefanía Guerrero Martin  
Universidad San José

SALINÓPOLIS-PA  
2025

## AGRADECIMENTOS

Sobre todas as coisas, agradeço a Deus, pois sem sua infinita bondade e misericórdia eu não conseguiria realizar essa conquista. A minha família; minha avó, meu pai, minha mãe, meu padrasto, minha irmã e meu noivo, que são os pilares da minha vida e sempre me incentivaram a buscar nos estudos o melhor.

Minha gratidão a todas as pessoas que fizeram eu alcançar essa conquista de forma direta ou indireta. A biblioteca do campus onde pude trabalhar ao lado de pessoas comprometidas que levarei para toda vida, meus muito obrigada Sheysy Aragão, Fernanda Nara, Clicia e Fabio. Aos amigos e colegas do Campus Salinópolis o qual orgulho-me de ter feito parte, meu respeito, admiração e felicidades para com todos.

Em especial, agradeço à equipe da ANP, onde tive minha primeira experiência no setor de Óleo & Gás. Sou profundamente grata por todo o conhecimento compartilhado e pela forma como a SSO está sempre disposta a incluir e transmitir saber aos futuros profissionais da área que atuam hoje como estagiários. Minha eterna gratidão a todos que passaram e deixaram um conhecimento técnico ou profissional que me afetou de certa forma, incluindo a equipe de Sondas e Poços que terá um lugar especial no meu coração. Aos colegas mais próximos, meu sincero agradecimento: Muriel Cortez Guerrero, Alberto Rodamilans Freire de Carvalho, Marcos André Rodrigues Alves (Marcola), Anderson do Santos Abreu, Rafael Couto de Albuquerque, Luciano da Silva Pinto Teixeira, Natanael Rodrigues de Souza, Carlos Alexandre Silva Pedroto, Gabriel Saadi Rebello, Monique Fonseca de Resende, Celso Fraga da Silva, Elson Menezes Correia, Luiz Henrique de Oliveira Bispo, Thiago da Silva Ormonde e ao Antônio, Eduardo, Marquês e Ricaldi, sem vocês minha trajetória profissional talvez tivesse seguido outro rumo, e eu não teria descoberto minha paixão pela Segurança Operacional.

Gratidão ao Laboratório de Operações e Tecnologias Energéticas (LOTEP), onde desenvolvi minhas primeiras pesquisas e trabalhos científicos e pude adquirir experiências únicas dentro da graduação, inclusive este TCC. E por fim, agradeço ao meu orientador, Prof. Camilo Guerrero Martin, que me acolheu e cedeu a minha primeira oportunidade de desenvolver um trabalho científico, tens um coração enorme e sou grato por todas oportunidades recebidas.

## **ABSTRACT**

This study evaluates the techno-economic performance of a tidal energy project using the Tidal module of the System Advisor Model (SAM). The configuration corresponds to an array-scale installation with a total installed capacity of 1,115 kW. Under the site-specific resource and availability assumptions used in SAM, the model estimates an annual energy production of 212,946 kWh, yielding a capacity factor of 2%. The levelized cost of energy (LCOE) is calculated at 1,449.65 ¢/kWh. A detailed cost decomposition indicates total capital expenditures (CapEx) of \$15,971,341.37 (14,324 \$/kW), of which device hardware accounts for \$4,826,559.72 (4,329 \$/kW) and balance-of-system for \$9,330,683.69 (8,368 \$/kW), with financing charges of \$1,814,097.96 (1,627 \$/kW). Operations and maintenance (O&M) are projected at \$1,362,080.09 per year (1,222 \$/kW/yr). In LCOE terms, the contributions are 2.45 \$/kWh (devices), 4.73 \$/kWh (balance of system), 0.92 \$/kWh (financial), and 6.40 \$/kWh (O&M), with the remainder attributable to capital recovery. The results highlight the sensitivity of LCOE to capacity factor and O&M intensity: the low modeled capacity factor drives limited energy yield against high fixed costs, while O&M dominates recurring costs. Implications for design and project development include prioritizing resource characterization and device availability, optimizing array sizing and layout to increase capacity utilization, and reducing installation and maintenance logistics to compress both BOS and O&M burdens. These insights can guide subsequent parametric studies within SAM to identify scenarios that materially improve cost competitiveness.

**Keywords:** Tidal energy; System Advisor Model (SAM); techno-economic analysis; capacity factor; levelized cost of energy (LCOE); capital expenditure (CapEx); operations and maintenance (O&M); device array; balance of system (BOS); renewable marine energy.

## SUMÁRIO

|               |   |           |
|---------------|---|-----------|
| <b>1.</b>     | <b>INTRODUCTION .....</b>                                   | <b>1</b>  |
| <b>2.</b>     | <b>THEORETICAL BACKGROUND .....</b>                         | <b>2</b>  |
| <b>3.</b>     | <b>METHODS.....</b>   | <b>4</b>  |
| <b>3.1.</b>   | <b>General information and field of study .....</b>         | <b>4</b>  |
| <b>3.2.</b>   | <b>Data Acquisition .....</b>                               | <b>5</b>  |
| <b>3.3.</b>   | <b>Techno-economic simulation method (SAM — Tidal).....</b> | <b>7</b>  |
| <b>3.3.1.</b> | <b>Resource input and pre-processing .....</b>              | <b>7</b>  |
| <b>3.3.2.</b> | <b>Device and array configuration .....</b>                 | <b>8</b>  |
| <b>3.3.3.</b> | <b>Electrical collection and export .....</b>               | <b>8</b>  |
| <b>3.3.4.</b> | <b>Cost model parameterization (CAPEX) .....</b>            | <b>8</b>  |
| <b>3.3.5.</b> | <b>Operations and maintenance (fixed annual) .....</b>      | <b>9</b>  |
| <b>3.3.6.</b> | <b>LCOE calculator settings .....</b>                       | <b>10</b> |
| <b>3.3.7.</b> | <b>Computational workflow and outputs .....</b>             | <b>10</b> |
| <b>4.</b>     | <b>RESULTS AND DISCUSSION.....</b>                          | <b>11</b> |
| <b>5.</b>     | <b>CONCLUSION .....</b>                                     | <b>16</b> |
|               | <b>REFERENCES .....</b>                                     | <b>17</b> |

## 1. INTRODUCTION

The exploration process in the oil and gas industry faces several challenges related to drilling, production, and the transportation of hydrocarbons (Katysheva & Tsvetkova, 2019). This transport is usually carried out through subsea pipelines interconnected with a gathering unit. These pipelines must provide low internal resistance to facilitate fluid flow and sufficient external strength to withstand environmental conditions (Araújo & Moura, 2017).

The transported fluid is a three-phase mixture of water, oil, and gas. When this mixture is exposed to low temperatures, these components can solidify, forming hydrates and deposits inside the pipelines; as this material accumulates, it can obstruct the lines and impede fluid flow (Fraga, 2017). The blockage of the fluid pathway represents a significant challenge and can lead to delays in production and transport, as loss of flow occurs when obstruction develops (Da Silva, 2015).

In view of these transport challenges, several technologies have been developed to facilitate the process. An important technique to consider is the use of PIP (pipe-in-pipe) systems, which offer excellent thermal-insulation properties. A PIP system consists of an inner pipe that carries hydrocarbons and an outer pipe that supports the hydrostatic pressure of the environment. The annular space between the pipes provides thermal resistance, effectively preventing the formation of hydrates (Souza, 2008; Euphemio et al., 2004).

One way to supply the energy required for resistive heating in the pipeline annulus is to use electricity. However, to reduce long-term operating costs, an alternative approach is to power the system with renewable energy sources (Costa & Prates, 2005). The oil industry is increasingly integrating renewables into its production and transport processes (upstream and downstream). In this context, wave energy emerges as an option, enabling power generation by harnessing wave motion (Dantas, 2015). The electricity generated from ocean waves can be applied to various systems, including pipeline heating, thereby avoiding hydrate formation (Ribeiro et al., 2007).

By incorporating renewable energy sources, the oil industry can improve the efficiency and sustainability of its operations while simultaneously reducing long-term operating costs and lowering emissions of polluting gases that have major environmental impacts. These changes can be crucial for advancing techniques used in resource exploitation, decreasing the use of non-renewables by repurposing existing technologies for renewable-energy generation (Lamiz et al., 2014).

The importance of this study lies in implementing devices that capture wave energy and convert it into electricity to supply pipeline systems. This work offers a new perspective on using renewable energy in the oil industry, moving closer to the long-awaited energy transition. The objective is to assess the feasibility and effectiveness of using wave energy as a sustainable solution to prevent hydrate formation in these pipelines.

## **2. THEORETICAL BACKGROUND**

Oil and gas are among the most widely exploited raw materials in the world, with uses dating back before the fourteenth century. Initially, petroleum products were extensively used in maritime applications such as sealing vessels, road paving, and even as flammable components in naval warfare. In 1847, the first petroleum refinery was established in Baku, highlighting the evolution in the material's use, extending to public lighting through the production of kerosene from petroleum, which gained ground over other fuels (Morais, 2013; Macini & Mesini, 2018; Machado & Carvalho, 2021).

Over time, the demand for kerosene led to increased oil production since, compared with coal oil and whale oil, it was economically more viable—especially given the decline in whale populations (Lucchesi, 1998; Martins et al., 2015; Sauer, 2016). Subsequent studies underscored petroleum's diverse functionalities, particularly as a carbon- and hydrogen-based fuel (Prauchner et al., 2023; Li, H., et al., 2025).

Today, oil is the world's most important fuel source. Its high value has enabled the spread and evolution of production processes. Although oil is a finite resource, there is still significant exploration effort in this sector, with increasingly accurate, precise, and effective extraction technologies. Among the leading oil-producing countries in 2022, the United States stood out with total production of 17,770 thousand barrels/day (18.9%), followed by Saudi Arabia (12.9%), Russia (11.9%), Canada (5.9%), and others (Viana, 2024).

Hydrocarbon reserve development involves geology, geophysics, and drilling techniques. Among the different approaches, onshore operations rely on technologies that operate on land. This activity is widely practiced in China (e.g., in wind-energy fields) and in the United States for oil and natural gas; in 2019, the United States reached production of 12.2 million b/d from onshore systems using modern technology. In Brazil, this exploratory model accounts for only 2.4% and 12.8%, respectively (Schutte & Debone, 2021; EPE, 2021). Offshore systems, in turn, are used to reach reserves on the seafloor, drawing on maritime

techniques to map and study locations, as well as constructing drilling platforms that access reservoirs at great depths. Brazil is among the world's top ten oil producers; the top three are the United States, Saudi Arabia, and Russia. According to Brazil's National Agency of Petroleum, Natural Gas and Biofuels, national production reached 4.666 million barrels of oil equivalent per day (MMboe/d), of which 97.6% and 87.2% of oil and natural gas, respectively, came from offshore fields (ANP, 2023; Ortiz Neto & Shima, 2008).

Offshore systems typically transport fluids via subsea lines connected or interconnected to a gathering unit, which is also responsible for maintaining and storing the extracted product until the next stages of the value chain (Chakrabarti, 1987). Fluid conduits must provide internal conditions conducive to flow and external resistance to physical and chemical variables (pressure, seawater temperature, and corrosive processes).

During transport, several issues can interrupt flow in the pipelines. Because the three-phase fluid (water, oil, gas) changes physically when exposed to lower temperatures along the route (Queiroz et al., 2019; Sousa et al., 2012), cooling can trigger physical reactions that cause solid compounds to precipitate (Araújo et al., 2017). These solids can deposit on inner walls, forming scale that hinders flow, increases hydraulic resistance, and reduces overall system efficiency (de Souza-Alves et al., 2023). To address these challenges, specific systems have been developed.

PIP (Pipe-in-Pipe) systems represent a technological evolution for subsea fluid transport. This concept installs an inner pipe within an outer pipe, creating an isolated annular space that limits or reduces interaction between the flowing fluid and the external environment (Zampirolli & Marques, 2020). The design provides thermal benefits by minimizing heat loss during the transport of hot fluids, as well as mechanical benefits, improving resistance to external loads and corrosion (Wang et al., 2024; Bondarik et al., 2018). It is important that this structure be designed with durable materials, such as stainless-steel alloys and anti-corrosion coatings, to ensure long-term durability and structural integrity even in harsh marine environments.

However, these production processes consume large amounts of electricity, which often entails burning fossil fuels and emitting CO<sub>2</sub>. The oil and gas industry therefore seeks to reduce reliance on non-renewables and to implement systems powered by renewable energy, enabling the deployment of different sources based on natural dynamics (Losekann & Hallack, 2018; Teixeira & Pessoa, 2024; Araújo et al., 2022). The idea is that systems like PIP can be

supplied—fully or partially—by renewable sources, further supporting more sustainable production and potentially lowering costs.

In the oil and gas industry, integrating renewables such as solar, wind, marine energy, and especially wave energy provides opportunities to tap alternative power sources that can be both productive and economically viable, primarily because the necessary resources are available on site (Zakariazadeh et al., 2024; De Oliveira et al., 2018). Installation costs can be offset by reduced reliance on non-renewables, yielding financial savings and more sustainable operations (Rossi et al., 2024; Pereira et al., 2019).

The intention is to create hybrid systems that combine renewable generation with conventional oil and gas facilities to optimize operational efficiency and bridge supply gaps (Bamisile et al., 2024). In offshore platforms, environmental resources—particularly the ocean—offer opportunities to install power-generation systems.

Given the locations of offshore platforms, wave energy is a promising renewable option, using the dynamics of wave motion to generate electricity. Technologies include turbines that harness mechanical wave motion and other ocean-energy conversion systems to extract energy from wave run-up and backwash (Costa & das Neves Gomes, 2024).

One such technology is the Oscillating Water Column (OWC), which uses the oscillation of seawater to drive a turbine and generate electricity. This highlights the diversity of approaches to capturing renewable energy from ocean waves (De Oliveira et al., 2017; Deus et al., 2019; Zhao & Ning, 2024). A sound scientific basis is essential to determine the real value of such systems, analyzing their potential and, above all, their benefits for drilling and production systems (Zhao et al., 2024).

### **3. METHODS**

#### **3.1. General information and field of study**

The methodology consists of assessing the energy potential generated by a system that converts mechanical energy from variations in the water column into electricity, with the aim of heating pipe-in-pipe systems to prevent hydrate formation and deposits that reduce the flow of recovered hydrocarbons. According to Vennell (2012), hydrates can form at temperatures up to 36.85 °C. The simulations in this study use the System Advisor Model (SAM), version 2022.11.21, developed by the National Renewable Energy Laboratory (NREL).

O The study area lies within the Pará–Maranhão Basin, where four points were selected forming a quadrilateral along the equatorial margin. The selected coordinates (latitude, longitude) are: (LAT: 0.095, LONG: -38.714), (LAT: -0.240, LONG: -38.052), (LAT: -0.651, LONG: -38.186), and (LAT: -0.375, LONG: -38.831).

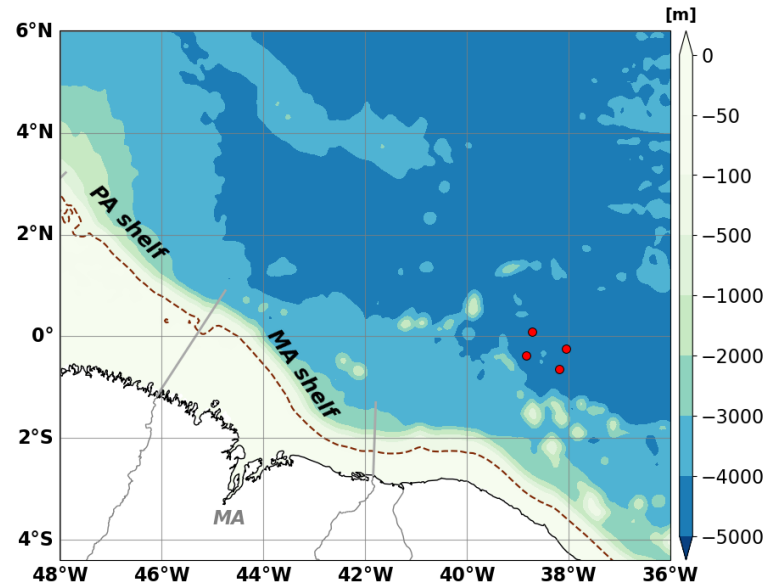


**Figura 1.** Study area in the Pará–Maranhão Basin.

Data was extracted from the Copernicus Marine Service to obtain the potential temperature of seawater at the four points mentioned. The results indicate temperatures with a high potential for deposit formation (See Table 1.).

Table 1. Temperature and Depth.

| Temperature (°C) | Depth (m) |
|------------------|-----------|
| 27,74535         | 1,541375  |
| 26,7292          | 55,76429  |
| 21,55299         | 109,7293  |
| 18,69008         | 130,666   |
| 15,86047         | 155,8507  |
| 12,59685         | 222,4752  |
| 10,75081         | 318,1274  |

### 3.2. Data Acquisition

Most data were obtained from the Copernicus Marine Service, specifically the Global Ocean Physics Analysis and Forecast product, which provides daily and monthly mean files of temperature, salinity, currents, sea level, mixed-layer depth, and ice parameters. It also offers a special surface-current dataset that includes wave and tide drift, known as SMOC (Surface Merged Ocean Current).

By selecting four points of interest on the map (latitude and longitude), the product returns several model outputs. Four orthogonal components were chosen to support the analysis: east–west current velocity ( $u$ ), north–south current velocity ( $v$ ), and ocean potential temperature ( $\theta$ ) for the period 01/2021 to 12/2023.

Characterize the local hydrodynamic regime, we computed the horizontal current speed magnitude as  $|V| = \sqrt{u^2 + v^2}$  from the Copernicus  $u$  (east–west) and  $v$  (north–south) components at the four selected coordinates for the 2021–2023 period. The resulting time series were aggregated into a normalized frequency histogram (Figure X). The distribution is dominated by moderate currents ( $\approx 0.3$ – $0.7$  m/s) with a clear right-skew and a low incidence of events  $> 1.5$  m/s. This velocity climatology complements the temperature and stratification data, providing (i) context for convective heat-loss conditions relevant to PIP thermal performance and hydrate risk, and (ii) a quality-control check on the marine forcing used later in the resource and heating simulations (see Figure 2). Because  $u$  (along-shelf) and  $v$  (cross-shelf) are orthogonal components of current velocity, the current speed magnitude is the square root of the sum of the squares of  $u$  and  $v$ . A Python script was written to compute this magnitude; the resulting data were saved as a CSV file for easier import and handling in SAM, which is subsequently used to simulate the energy available at the study points.

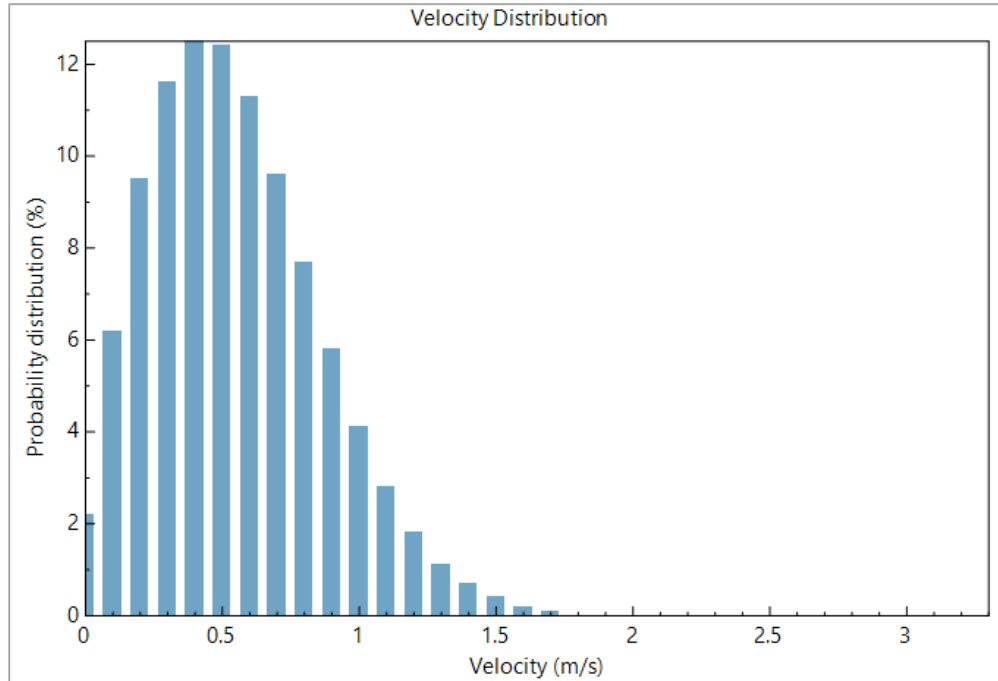


**Figure 2.** Velocity distribution at the study sites. Histogram of horizontal current speed (m/s) expressed as a percentage frequency. The distribution is right-skewed, with most observations between 0.3–0.7 m/s and a modal class around ~0.45–0.55 m/s (~12–13%). Speeds above 1.5 m/s are rare.

### 3.3. Techno-economic simulation method (SAM — Tidal)

The techno-economic assessment was conducted using the Tidal performance model of the National Renewable Energy Laboratory’s System Advisor Model (SAM, v2022.11.21). The workflow converts the site-specific current-speed resource into electrical output for a representative tidal device and then applies electrical architecture, capital and O&M costs, and financial assumptions to compute a screening-level levelized cost of energy (LCOE). All numerical inputs below correspond to the configuration shown in the provided SAM screenshots.

#### 3.3.1. Resource input and pre-processing

The resource supplied to SAM is the empirical probability distribution of horizontal current speed ( $\text{m s}^{-1}$ ) for the study area (Section 3.1). Current magnitude was computed from Copernicus east–west and north–south components as  $V = \sqrt{(u^2 + v^2)}$  over 2021–2023 and binned into a normalized histogram (Figure X). Under the Tidal module, when time series are not used, each speed bin is mapped to device power via the manufacturer power curve and aggregated by bin probability to estimate annual energy.

### 3.3.2. Device and array configuration

System sizing employed a single device, yielding a rated array capacity of 1,115 kW. The array layout was configured as one row with one device per row. Site parameters were distance to shore = 5,000 m, water depth = 50 m, and cable system overbuild = 10%. The “Floating array” and “Export cable redundancy” options were not enabled. This pilot-scale setup isolates device-level performance without inter-array interactions.

### 3.3.3. Electrical collection and export

Calculated cable lengths for the base case were inter-array = 0 m, export = 5,555 m, and riser = 0 m. Assumed AC cable voltages were 7.2 kV for inter-array, export, and riser circuits. Offshore and onshore substations were not required, the device exports directly to shore at the assumed medium voltage. In SAM, row spacing affects cable lengths but does not influence energy production for a single-device configuration.

### 3.3.4. Cost model parameterization (CAPEX)

SAM’s tidal cost framework was used with the option “Use Modeled Costs (\$)” for each category. The modeled values (USD) are reported in Tables 2–4. Table 5 summarizes the total capital cost used in the LCOE.

Table 2. Device Costs (Capital)

| Subcategory                        | Modeled value (USD) |
|------------------------------------|---------------------|
| Structural assembly                | \$1,314,290.00      |
| Power take-off (PTO) system        | \$2,633,386.00      |
| Mooring, foundation & substructure | \$878,883.00        |
| Total device costs                 | \$4,826,560.00      |

Table 3. Balance-of-System (BOS) Costs (Capital)

| Subcategory | Modeled value (USD) |
|-------------|---------------------|
| Development | \$3,126,698.00      |

|                              |                |
|------------------------------|----------------|
| Engineering & management     | \$2,412,629.00 |
| Electrical infrastructure    | \$885,871.00   |
| Plant commissioning          | \$62,555.00    |
| Site access / port / staging | \$84,140.00    |
| Assembly & installation      | \$2,758,791.00 |
| Other infrastructure         | \$0.00         |
| Total BOS costs              | \$9,330,684.00 |

Table 4. Financial Costs (Capital)

| Subcategory                   | Modeled value (USD) |
|-------------------------------|---------------------|
| Project contingency budget    | \$1,209,399.00      |
| Insurance during construction | \$151,175.00        |
| Reserve accounts              | \$453,524.00        |
| Other financial costs         | \$0.00              |
| Total financial costs         | \$1,814,097.00      |

### 3.3.5. Operations and maintenance (fixed annual)

Table 5. Fixed Operations & Maintenance (Annual)

| Subcategory     | Modeled value (USD / year) |
|-----------------|----------------------------|
| Operations      | \$914,126.00               |
| Maintenance     | \$447,954.00               |
| Total fixed O&M | \$1,362,080.00             |

### 3.3.6. LCOE calculator settings

SAM's fixed-charge-rate (FCR) method was used for a screening-level LCOE estimate. The parameters used by the calculator are summarized in Table 6. The analytical expression is (Equation 1):

$$\text{LCOE} = (\text{FCR} \times \text{Capital cost} + \text{Fixed operating cost}) / \text{Annual Energy} + \text{Variable operating cost}$$
 (Equation 1).

Table 6. CAPEX Summary (input to LCOE)

| Category                | Amount (USD)    |
|-------------------------|-----------------|
| Total device costs      | \$4,826,560.00  |
| Total BOS costs         | \$9,330,684.00  |
| Total financial costs   | \$1,814,097.00  |
| Total capital cost (CC) | \$15,971,341.37 |

Table 7. LCOE Calculator Inputs (FCR method)

| Parameter                     | Value                 |
|-------------------------------|-----------------------|
| System capacity               | 1,115 kW              |
| Capital cost (CC)             | \$15,971,341.37       |
| Fixed operating cost (FOC)    | \$1,362,080.09 / year |
| Variable operating cost (VOC) | \$0.00 / kWh          |
| Fixed charge rate (real, FCR) | 0.108 (10.8%)         |

### 3.3.7. Computational workflow and outputs

1) Import the velocity histogram for the four study coordinates; 2) configure the single 1.115-MW device and base layout; 3) set electrical collection/export parameters and voltages as above; 4) apply modeled Device, BOS, Financial, and O&M costs; 5) run the Tidal

performance simulation to obtain annual energy (AEP), net AC power, and capacity factor; 6) compute economic performance with the LCOE calculator using the specified FCR, CC, and FOC. The resulting energy and cost metrics are subsequently coupled to the pipe-in-pipe resistive-heating analysis to quantify the renewable share of the heating load and any residual auxiliary power requirement.

#### 4. RESULTS AND DISCUSSION

The conversion of the site’s current-speed statistics into energy follows the familiar resource–device interplay: when the empirical velocity distribution is mapped through the turbine’s power curve, annual yield accumulates primarily in the bins that coincide with the modal currents, while the tails contribute little. This behavior is explicit in the Annual Energy Production by velocity bin (Figure 3), where production climbs from the lowest bins to a broad maximum in the mid-range (approximately bins 9–11) and then declines toward the high bins.

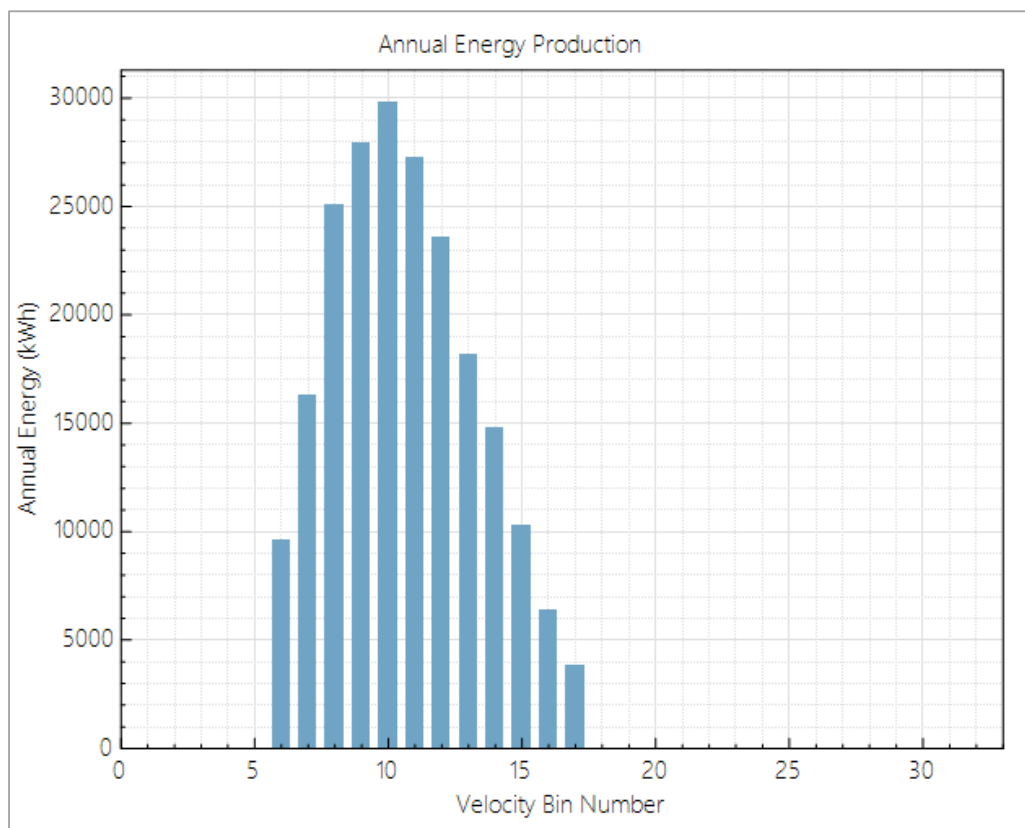


**Figure 3-** . Annual Energy Production by velocity bin — mid-range bins dominate.

The companion Cumulative Annual Energy Production (Figure 4) plateaus by around bin 18, confirming that infrequent high-speed events add only marginal energy over the year. In practical terms, this means that performance at this site is governed by capture in the mid-

speed band rather than by rare peaks; consequently, device characteristics that improve conversion efficiency, lower the cut-in threshold, or bring the onset of rated operation closer to the 0.3–0.7 m s<sup>-1</sup> regime will move the energy needle far more than enhancements aimed solely at very high currents.

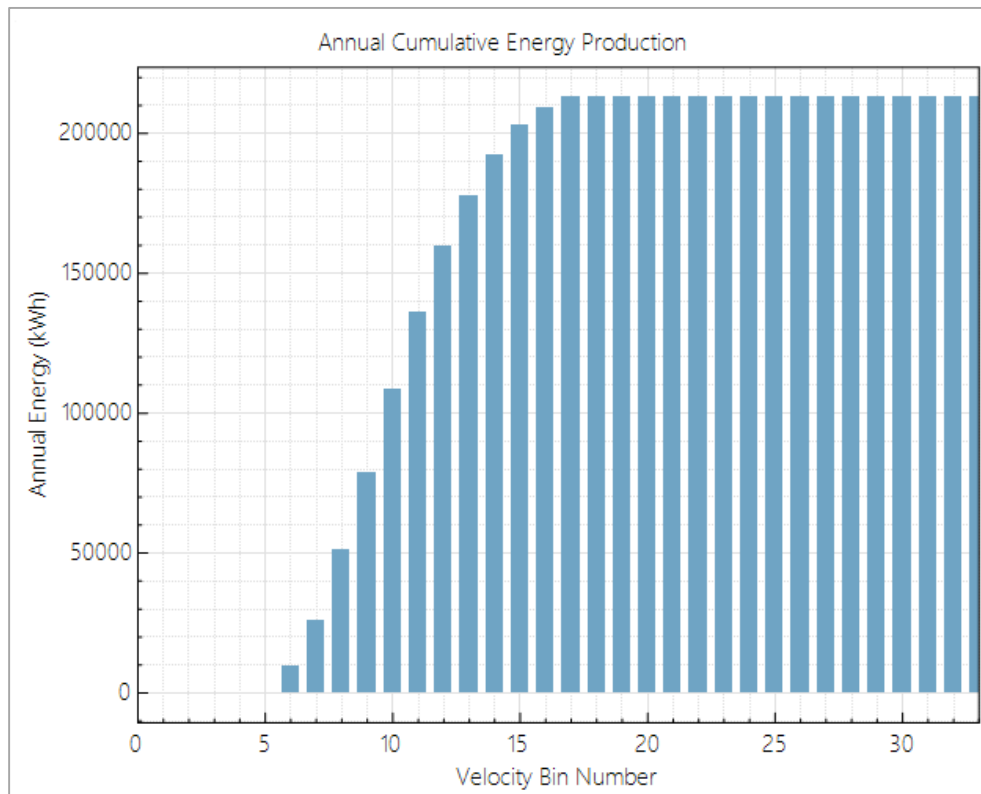


**Figure 4.** Annual Cumulative Energy Production — curve saturates by ~bin 18, confirming limited impact of rare high-speed events.

SAM’s Tidal model summarizes the production outcome as an annual energy of 212,946 kWh for the single-device configuration, with an average net output of 26 kW against an installed capacity of 1,115 kW. The implied utilization is therefore on the order of 2 %, consistent with the value reported in the software summary (Table 7). This low-capacity factor is not a modeling artifact but a direct reflection of the site–device mismatch: the speed climatology is dominated by moderate currents, so the machine spends most of the year operating well below its rating. The mid-bin dominance seen in Figure 1 corroborates this reading. From an operational perspective, a continuous average of roughly 26 kW can make a measurable contribution to resistive heating of a pipe-in-pipe (PIP) system—particularly for short tiebacks, segmented heating zones, or scenarios with strong insulation and modest environmental heat loss—yet it is unlikely to carry the full heating load of long lines in colder

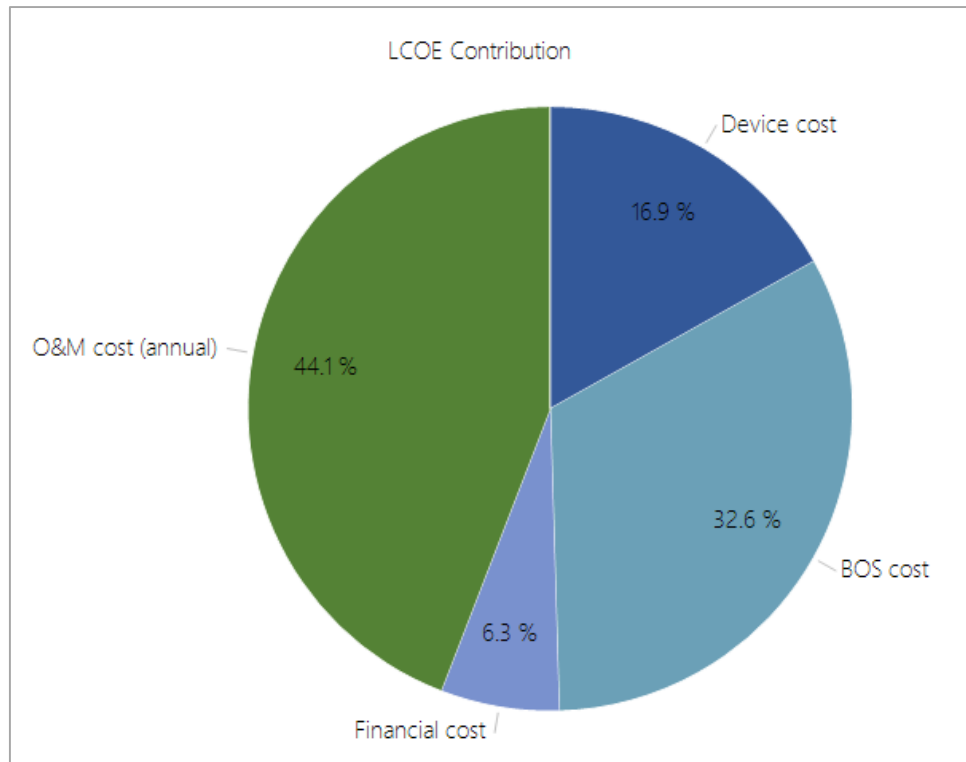
water without either scaling the array, hybridizing with grid/diesel power, or reducing thermal losses.

Table 8. Summary tables — AEP 212,946 kWh; average power 26 kW; capacity factor 2 %; capital cost \$15.97 M; O&M \$1.36 M/yr; LCOE 1,449.65 ¢/kWh; detailed cost intensities and per-category LCOE contributions.

| Item                            | Type   | Value         | Cost               | Cost per capacity | LCOE        |
|---------------------------------|--------|---------------|--------------------|-------------------|-------------|
| Annual energy production        | Metric | 212,946 kWh   |                    |                   |             |
| Average power per device        | Metric | 26 kW         |                    |                   |             |
| System capacity                 | Metric | 1,115 kW      |                    |                   |             |
| Capacity factor                 | Metric | 2 %           |                    |                   |             |
| LCOE (Levelized cost of energy) | Metric | 1449.65 ¢/kWh |                    |                   |             |
| Capital cost (total)            | Cost   |               | \$15,971,341.37    | 14,324 \$/kW      | 8.10 \$/kWh |
| Device cost                     | Cost   |               | \$4,826,559.72     | 4,329 \$/kW       | 2.45 \$/kWh |
| Balance of system cost          | Cost   |               | \$9,330,683.69     | 8,368 \$/kW       | 4.73 \$/kWh |
| Financial cost                  | Cost   |               | \$1,814,097.96     | 1,627 \$/kW       | 0.92 \$/kWh |
| O&M cost                        | Cost   |               | \$1,362,080.09 /yr | 1,222 \$/kW/yr    | 6.40 \$/kWh |

The economic outputs reinforce the same story. For the base case, SAM’s modeled capital cost is \$15,971,341.37 (about \$14,324 per kW), and the fixed O&M burden is \$1,362,080.09 per year; variable O&M is set to zero for screening. Using a real fixed charge rate of 10.8 %, the levelized cost of energy (LCOE) reported by the model is 1,449.65 ¢/kWh, roughly \$14.50/kWh (Figure 3). The LCOE decomposition makes clear where the pressure points lie: O&M accounts for 44.1 % of LCOE (about \$6.40/kWh), balance-of-system (BOS) capital for 32.6 % (\$4.73/kWh), device capital for 16.9 % (\$2.45/kWh), and financial capital for the remaining 6.3 % (\$0.92/kWh), as depicted in the pie chart (Figure 5). Two mechanisms drive these values. First, the energy denominator is small because of the low-capacity factor; large fixed charges—both the capital recovery and the annual O&M—are therefore spread over limited annual production. Second, the single-unit architecture forces lumpy BOS costs

(notably the 5.555 km export cable at 7.2 kV and the associated installation) to be carried by one device; the configuration deliberately avoids offshore/onshore substations to keep the electrical scheme simple, which is appropriate for a pilot but limits opportunities to optimize voltage, reduce cable cross-section, or share infrastructure across devices.



**Figure 5.** LCOE contribution pie chart — O&M 44.1 %, BOS 32.6 %, Device 16.9 %, Financial 6.3 %.

The figures also indicate cost intensities that are typical of early-stage deployments: approximately \$4,329/kW for device hardware, \$8,368/kW for BOS, \$1,627/kW for financial capital, and \$1,222/kW per year for fixed O&M (Figure 3). In a commercial multi-device context these values generally compress as installation logistics, export architecture, spare parts, and maintenance resources are shared across units, and as higher export voltages and subsea hubs reduce per-device cable length and losses. The strong mid-bin signal in Figure 1 suggests an additional lever: re-rating the device to bring cut-in and rated operation closer to the prevailing speeds or selecting a turbine with greater swept area per unit capacity and a power curve optimized for moderate flows. Either approach raises the time spent in the machine's high-efficiency region and can lift annual energy substantially without changing site conditions.

For the PIP heating application, these results imply a clear strategy. If the heating system is designed to accept variable renewable supply—through duty-cycling of the cable,

segmentation of heated lengths, and priority dispatch of tidal power whenever available—the single device can offset a meaningful share of the electrical load in benign segments. Where the thermal margin is tight or the heat loss per unit length is high, the base case will under-deliver; the appropriate response is not only to add auxiliary power, but also to attack the root causes by reducing the overall heat-transfer coefficient (better insulation or annulus design), shortening exposed lengths, and, if the marine resource allows, micro-siting to slightly more energetic corridors or adjusting hub height to benefit from vertical shear without compromising clearances. Because the Cumulative AEP flattens well before the highest velocity bins, incremental improvements that increase the frequency with which the device operates in the mid-range—through siting, rotor and control choices, or modest speed gains—will yield outsized energy returns relative to efforts targeted at rare high-speed events.

Finally, it is important to situate these numbers within their modeling context. The assessment uses SAM’s default tidal cost framework and a statistical resource input derived from binned speeds rather than a full time series. Uncertainty therefore stems from manufacturer-specific power curves and availability assumptions, year-to-year variability in currents and possible differences between measurement depth and hub height, site-specific installation practices, and the simplifying electrical architecture of a pilot. Those caveats notwithstanding, the results are internally consistent with the hydrodynamic evidence provided by the velocity-resolved energy plots: moderate currents dominate production; the single device’s utilization remains low; and, as a result, LCOE is driven more by fixed O&M and BOS than by device hardware. The path to technical and economic improvement is correspondingly clear—match the machine to the modal resource, scale to share infrastructure and reduce O&M intensity and re-optimize export architecture—after which the same modeling chain can be rerun to quantify gains in both annual energy and cost of energy for the PIP heating duty.

## 5. CONCLUSION

Energy is governed by moderate currents. The velocity-resolved results show that annual yield is concentrated in mid-speed bins; rare high-speed events add little to the total. This confirms that the site's resource is dominated by moderate flows and that performance hinges on conversion efficiency in that band.

Utilization is low for the base configuration. With AEP = 212,946 kWh, average net power  $\approx 26$  kW, and installed capacity = 1,115 kW, the capacity factor is  $\sim 2\%$ . This reflects a mismatch between the turbine's operating window and the prevailing speeds, not a modeling artifact.

Economics are driven by fixed charges. The modeled capital cost is \$15.97 M and fixed O&M \$1.36 M/yr; the LCOE is  $\sim \$14.5/\text{kWh}$ . The LCOE decomposition indicates that O&M (44.1%) and BOS capital (32.6%) dominate, with device capital (16.9%) and financial costs (6.3%) contributing less—consistent with a single-device pilot carrying lumpy export and installation costs.

Implications for PIP heating. A continuous mean supply of  $\sim 26$  kW can offset a limited fraction of resistive heating demand—potentially useful for short or segmented lines with good insulation—but is unlikely to meet full heating requirements for long tiebacks or colder water columns without additional measures.

Bottlenecks are identifiable and tractable. The principal constraints are (i) resource–device mismatch, (ii) lack of scale (single device), and (iii) a minimalist electrical/export architecture that cannot share costs or reduce per-kW BOS and O&M.

## REFERENCES

- ANP – Agência Nacional do Petróleo, Gás Natural e Biocombustíveis. (2023). Anuário estatístico 2023. ANP.
- Araújo, A. C. de, & Moura, R. D. de. (2017). *Análise de estabilidade hidrodinâmica de dutos submarinos pelo critério de estabilidade generalizada* [Manuscrito no publicado].
- Araújo, M. N., De Mattos, L. C. N., Fortunato, T. B., Dutra, J. C. S., & Da Silva, W. B. (2017). Monitoramento da temperatura de óleo em um sistema de tubulação multicamadas utilizando filtro bayesiano ASIR. *Engevista*, 19(3), 792. <https://doi.org/10.22409/engevista.v19i3.910>
- Araújo, R. S. de, Sousa, F. L. N. de, Vanderley, P. S., Bentes, S. O. da S., Gomes, L. M., & Ferreira, F. C. L. (2022). Fontes de energias renováveis: Pesquisas, tendências e perspectivas sobre as práticas sustentáveis. *Research, Society and Development*, 11(11), e468111133893. <https://doi.org/10.33448/rsd-v11i11.33893>
- Bamisile, O., Cai, D., Adun, H., Dagbasi, M., Ukwuoma, C. C., Huang, Q., & Johnson, N. (2024). Towards renewables development: Review of optimization techniques for energy storage and hybrid renewable energy systems. *Heliyon*, 10(19), e37482.
- Bondarik, R., Pilatti, L. A., & Horst, D. J. (2018). Uma visão geral sobre o potencial de geração de energias renováveis no Brasil. *Interciencia*, 43(10), 680–688.
- Chakrabarti, J. K. (1987). *Hydrodynamics of offshore structures*.
- Costa, R. C. da, & Prates, C. P. T. (2005). *O papel das fontes renováveis de energia no desenvolvimento do setor energético e barreiras à sua penetração no mercado*.
- Costa, R., & das Neves Gomes, M. (2024). Estudo bibliométrico da produção científica sobre conversores de energia das ondas do mar. *Revista Thema*, 23(2), 373–389.
- Dantas, C. E. B. (2015). *Estudo dos conversores de energia ondomotriz em energia elétrica*.
- Da Silva, G. S. (2015). Corrosão: Colunas de perfuração de poços de petróleo. *Caderno de Graduação – Ciências Exatas e Tecnológicas – UNIT – Alagoas*, 3(1), 65–74.
- De Carvalho, B. B. N. (2022). Autossuficiência elétrica em plataformas petrolíferas através da geração de energia eólica offshore. *Biblioteca de Monografias*, 1(001).
- De Oliveira, A. P. M., Fuganholi, N. S., Cunha, P. H. de S., Barelli, V. A., Bunel, M. P. M., & Novazzi, L. F. (2018). Análise técnica e econômica de fontes de energia renováveis. *The Journal of Engineering and Exact Sciences*, 4(1), 0163–0169. <https://doi.org/10.18540/jcecv14iss1pp0163-0169>
- De Oliveira, S. S., Oleinik, P. H., Gomes, M. das N., Dos Santos, E. D., Souza, J. A., Rocha, L. A. O., Marques, W. C., & Isoldi, L. A. (2017). Modelagem computacional de um conversor de

energia das ondas do tipo coluna de água oscilante (CAO) considerando dados de estado do mar. *Scientia Plena*, 13(4). <https://doi.org/10.14808/sci.plena.2017.049915>

Deus, M. J. de, Santos, E. D., Isoldi, L. A., Rocha, L. A. O., & Gomes, M. das N. (2019). Análise numérica da profundidade de submersão de um dispositivo coluna de água oscilante submetido a um espectro de ondas do tipo Pierson–Moskowitz. *Scientia Plena*, 15(4). <https://doi.org/10.14808/sci.plena.2019.049910>

EPE – Empresa de Pesquisa Energética. (2021). *Experiências internacionais na regulação da indústria de óleo & gás* (Nota técnica). Ministério de Minas e Energia.

Euphemio, M., Montesanti, J. R., Bragança, E. J., Almeida, M. M. D., Coelho, E., Maia, A. R., & Peres, M. B. (2004). Electrically heated pipe-in-pipe system for hydrate prevention on the Campos Basin. [Trabalho apresentado].

Fraga, V. S. (2017). *Análise fluidodinâmica computacional do gradiente de temperatura e da estabilidade em dutos submarinos*.

Katysheva, E., & Tsvetkova, A. (2019). Economic and institutional problems of the Russian oil and gas complex digital transformation. *International Multidisciplinary Scientific GeoConference: SGEM*, 19(5.3), 203–208.

Lamiz, M., da Rocha, P. M., Peres, R., Prado, V., & Gomes, C. F. S. (2014). Cenários prospectivos para a indústria petrolífera nacional: Planejamento de ações estratégicas para uma empresa exploradora e produtora. *Relatórios de Pesquisa em Engenharia de Produção*, 14(A17), 224–245.

Li, H., Shi, X., Kong, W., Kong, L., Hu, Y., Wu, X., ... & Yan, J. (2025). Advanced wave energy conversion technologies for sustainable and smart sea: A comprehensive review. *Renewable Energy*, 238, 121980.

Losekann, L., & Hallack, M. (2018). Novas energias renováveis no Brasil: Desafios e oportunidades. In J. A. D. Negri, B. C. Araújo, & R. Bacelette (Eds.), *Desafios da nação: Artigos de apoio* (Vol. 2, pp. 631–655).

Lucchesi, C. F. (1998). Petróleo. *Estudos Avançados*, 12(33), 17–40. <https://doi.org/10.1590/S0103-40141998000200003>

Macini, P., & Mesini, E. (2018). History of petroleum and petroleum engineering. In *Petroleum Engineering—Upstream* (Vol. 4).

Machado, J. D. de O. A., & Carvalho, R. A. de. (2021). Exploração de petróleo no Brasil e Estados Unidos: História e relevância. *Brazilian Journal of Development*, 7(5), 52499–52515.

Martins, S. S. da S., Azevedo, M. O. de, Silva, M. P. da, & Silva, V. P. da. (2015). Produção de petróleo e impactos ambientais: Algumas considerações. *HOLOS*, 6, 54. <https://doi.org/10.15628/holos.2015.2201>

Morais, J. M. de. (2013). *Petróleo em águas profundas: Uma história tecnológica da Petrobras na exploração e produção offshore*.

Ortiz Neto, J. B., & Shima, W. T. (2008). Trajetórias tecnológicas no segmento offshore: Ambiente e oportunidades. *Revista de Economia Contemporânea*, 12(2), 301–332. <https://doi.org/10.1590/S1415-98482008000200005>

Pereira, J. D. F., Neto, P. B. L., Saavedra, O. R., Torres, A. R., & Dias, F. J. S. (2019). Operação econômica de um sistema de autoprodução de energia baseada em correntes de maré considerando sistema de armazenamento. *Congresso Brasileiro de Automática – CBA*, 1(1). <https://doi.org/10.20906/CBA2022/223>

Prauchner, M. J., Brandão, R. D., Freitas Júnior, A. M. de, & Oliveira, S. da C. (2023). Petroleum-based fuels: Obtaining, properties and uses. *Revista Virtual de Química*, 15(1), 43–60. <https://doi.org/10.21577/1984-6835.20220073>

Queiroz, H. R., Azevedo Junior, G. M., Bentes, F. M., Nóbrega, M. de J. R., & Fattorillo, F. (2019). Sistemas marítimos de produção de petróleo: Um exemplo de interdisciplinaridade do ciclo básico das engenharias. *Brazilian Journal of Development*, 5(9), 17157–17168. <https://doi.org/10.34117/bjdv5n9-236>

Ribeiro, R. D., de Carvalho Pinheiro, B., & Paranhos, I. (2007). *Estudo da pressão de colapso em dutos sanduíches danificados*.

Rossi, V. S. L., Triches, D., Camargo, M. E., da Motta, M. E. V., & Priesnitz, M. C. (2024). As energias renováveis para o desenvolvimento sustentável organizacional. *Revista de Gestão e Secretariado*, 15(1), 1550–1566. <https://doi.org/10.7769/gesec.v15i1.3436>

Sauer, I. L. (2016). O pré-sal e a geopolítica e hegemonia do petróleo face às mudanças climáticas e à transição energética. In A. J. Melfi, A. Misi, D. de A. Campos, & U. G. Cordani (Eds.), *Recursos minerais do Brasil* (pp. 308–322).

Schutte, G. R., & Debone, V. S. (2021). Trajetória e desafios da matriz energética chinesa. *Revista Economia e Políticas Públicas*, 4(1), 111–134.

Sousa, B. V. P., Santos, F. C. de O. N., Rodrigues, F. C., Santos Filho, M. C. dos, Souza, M. V. C. S., Feitosa, P. H., Dias, Y. M. S., & Silva, M. de J. (2012). Perfurações de poços de petróleo: Métodos e equipamentos utilizados. *Caderno de Graduação – Ciências Exatas e Tecnológicas – UNIT – Sergipe*, 1(1), 103–108.

Souza, A. R. (2008). *Resistência estrutural de dutos sanduíche sob pressão externa, flexão longitudinal e carregamento térmico* (Dissertação de mestrado). COPPE/UFRJ.

Teixeira, R. L. P., & Pessoa, Z. S. (2024). Energias renováveis e mudanças climáticas: Análise de políticas públicas correlatas em estados do Nordeste brasileiro. *Ambiente & Sociedade*, 27, e00055. <https://doi.org/10.1590/1809-4422asoc00551vu27L4E23P>

Vennell, R. (2012). A energética de grandes conjuntos de turbinas de marés. *Energia Renovável*, 48, 210–219.

Viana, F. L. E. (2024). *Petróleo e gás natural*. *Caderno Setorial ETENE*, 9(351).

Wang, X., Yuan, L., Xu, P., Ding, Z., Wang, Y., & Gong, S. (2024). Evaluation of dynamic behaviour of pipe-in-pipe systems for deepwater J-lay method. *Applied Ocean Research*, 153, 104229. <https://doi.org/10.1016/j.apor.2024.104229>

Zakariazadeh, A., Ahshan, R., Al Abri, R., & Al-Abri, M. (2024). Renewable energy integration in sustainable water systems: A review. *Cleaner Engineering and Technology*, 100722.

Zampirolli, B. S., & Marques, R. de A. (2020). Modelos tridimensionais aplicados à engenharia de plataformas de petróleo offshore: Etapas de perfuração e riscos ambientais. *The Journal of Engineering and Exact Sciences*, 6(5), 0668–0681. <https://doi.org/10.18540/jcecvl6iss5pp0668-0681>